Properties of knotted ring polymers. II. Transport properties

ARTICLE *in* THE JOURNAL OF CHEMICAL PHYSICS · JULY 2010

Impact Factor: 2.95 · DOI: 10.1063/1.3457161 · Source: PubMed

2 AUTHORS:

Marc L Mansfield
Utah State University
85 PUBLICATIONS **1,973** CITATIONS
SEE PROFILE

J. F. Douglas
National Institute of Standards and Technolo…
428 PUBLICATIONS **14,795** CITATIONS
SEE PROFILE

Properties of knotted ring polymers. II. Transport properties

Marc L. Mansfield[1,a)] and Jack F. Douglas[2,a)]
[1]*Department of Chemistry, Chemical Biology, and Biomedical Engineering, Stevens Institute of Technology, Hoboken, New Jersey 07030, USA*
[2]*Polymers Division, National Institute of Standards and Technology, Gaithersburg, Maryland 20899, USA*

(Received 27 January 2010; accepted 3 June 2010; published online 27 July 2010)

We have calculated the hydrodynamic radius R_h and intrinsic viscosity $[\eta]$ of both lattice self-avoiding rings and lattice theta-state rings that are confined to specific knot states by our path-integration technique. We observe that naive scaling arguments based on the equilibrium polymer size fail for both the hydrodynamic radius and the intrinsic viscosity, at least over accessible chain lengths. (However, we do conjecture that scaling laws will nevertheless prevail at sufficiently large N.) This failure is attributed to a "double" cross-over. One cross-over effect is the transition from delocalized to localized knotting: in short chains, the knot is distributed throughout the chain, while in long chains it becomes localized in only a portion of the chain. This transition occurs slowly with increasing N. The other cross-over, superimposed upon the first, is the so-called "draining" effect, in which transport properties maintain dependence on local structure out to very large N. The hydrodynamic mobility of knotted rings of the same length and backbone structure is correlated with the average crossing number X of the knots. The same correlation between mobility and knot complexity X has been observed for the gel-electrophoretic mobility of cyclic DNA molecules. © *2010 American Institute of Physics*. [doi:10.1063/1.3457161]

I. INTRODUCTION

Prokaryotic DNA is an important physical example of a ring polymer. Through the action of topoisomerase and other enzymes, these DNAs can be prepared in a variety of knot states.[1–6] Each knot state proves to have a distinct electrophoretic mobility, which increases with knot complexity, and which permits separation of the DNAs by knot state.[7–13] One interesting empirical result, at conditions of low voltage in gels with large mesh sizes, is that the electrophoretic mobility of knotted DNAs is a linear function of a property known as the "average crossing number" of the knot, which we denote X.[8,14] X is, in turn, related to the concept of a "maximally inflated" knot. Imagine a knot modeled as a rope with finite thickness d and with contour length L. Then imagine transforming the structure either by increasing d at constant L ("inflating" the knot)[15] or by decreasing L at constant d.[16] The "maximally inflated" knot is that structure for which, for a given knot type, the ratio L/d achieves its global minimum. We also let p, the "rope length," represent the value of this global minimum: $p=[L/d]_{\min}$. If we then project the axial path of the maximally inflated structure onto an arbitrary plane, we obtain a two-dimensional closed curve which crosses itself. X is the mean number of crossings in these two-dimensional projections when averaged over projection planes of all possible orientations. It is distinct from the minimum crossing number C, defined as the minimum in the number of crossings with which any given knot state can be drawn, although obviously $X>C$. Values of p and X for many knots are tabulated,[14,17] and for convenience have been reproduced in the sequel paper[18] for the knots represented in this study.

Motivated in part by the linear relationship between DNA electrophoretic mobility and X, a number of research groups have computed transport properties of knotted ring polymers by several different techniques. These computations, summarized in the following paragraphs, have been performed using either (1) hydrodynamic theory at varying levels of sophistication or (2) dynamic Monte Carlo. The hydrodynamic calculations apply directly to solute particles in dilute solution, and it is not entirely clear that they are adequate for the electrophoretic mobility, although it is occasionally assumed that the electrophoretic gel constitutes an effective hydrodynamic medium. Dynamic Monte Carlo calculations are also deficient because they neglect hydrodynamic interactions. This neglect is especially serious in dilute solution, where it is known to give incorrect mass-scaling exponents for transport properties.[19,20] On the other hand, the neglect of hydrodynamic interactions may not be severe when modeling gel-electrophoretic transport, since hydrodynamic interactions are at least partially screened by the gel. As a further shortcoming, none of the computations are able to capture the subtleties of local electric field effects. To emphasize that hydrodynamic theories may be inadequate for gel-electrophoretic transport, we will make a distinction, in this work, between the "electrophoretic mobility" and the "hydrodynamic mobility."

Several requirements probably need to be satisfied before we could expect the hydrodynamic and electrophoretic mobilities to be proportional. One is that the gel possesses an effective viscosity, transferable from one solute particle to another, because the solvent viscosity is the only character-

a)Authors to whom correspondence should be addressed. Electronic addresses: marc.mansfield@stevens.edu and jack.douglas@nist.gov.

istic of the solvent which determines the hydrodynamic mobility of the solute. [See Eq. (1) below.] An effective viscosity might exist over a narrow range of particle sizes determined by the mesh size, but would probably break down when particles are either much smaller than the mesh size (the actual solvent viscosity then being relevant) or much larger than the mesh size (all large particles being trapped to the same extent by the gel with particle size becoming irrelevant). Another requirement is that the conformation of the particle be unperturbed by the gel, since conformational structure is unperturbed to first order in a hydrodynamic flow, and indeed the hydrodynamic radius [as defined in either Eq. (1), Eq. (2), or Eq. (3) below] is a purely geometrical property, determined only by the geometrical form of the solute particle, and by no other property of the solute.

Sheng and Tsao[21] estimated mobilities of lattice random knots by dynamic Monte Carlo, so that their approach suffers from the deficiencies mentioned above. Nevertheless, they report correlations between mobility and $p=[L/d]_{\min}$.

A number of authors have employed the Kirkwood double sum formula, which is probably the simplest hydrodynamic theory that still achieves a reasonably accurate description. It relates the mobility or diffusivity to the values $\langle 1/r_{ij}\rangle$ between pairs of segments at the surface of the particle, and sums these over all pairs of segments. However, it is known to systematically overestimate the mobility of any particle, and has been shown to be in error by as much as about 10% or 20% for several random-coil models.[22] Matuschek and Blumen[23] and Croxton and Turner[24] independently examined the mobility of knotted ring polymers using the double-sum formula. However, both groups essentially assumed tight knots with equally sized loops, which effectively convert the ring into a star polymer for which the termini are pairwise attached. This is inconsistent with what we now know about the conformations of knotted ring polymers. At low and moderate molecular mass, the knots are not tight. At sufficiently high molecular masses, they do become tight and localized, but these tight knots form with a single long loop, not with a series of equal-length loops.[15,18,25–30] Matuschek and Blumen examine ideal rings, while Croxton and Turner examine rings in good solvent, with swelling approximated through the iterative convolution technique of Croxton.[31] In another calculation, Stasiak *et al.*[8] estimated the mobility of maximally inflated knots in the Kirkwood double-sum approximation. They report a linear dependence of the mobility on X.

Hydrodynamic calculations that are more sophisticated than the Kirkwood double-sum formula can be performed by several different techniques. One approach, applicable to macromolecules with conformational flexibility, is the Zimm rigid-body approximation.[32] In such studies, the transport properties of an individual conformation are evaluated as if it were a rigid body, and then the results for an ensemble of conformations are averaged at the end. As pointed out by Zimm,[32] the rigid-body approximation is expected to be harmless as long as Brownian motion is dominant. This approach was applied by Vologodskii *et al.*[10,33] to random knotted polymers—or to be more precise, they obtained results for a relatively large ensemble of simulated chains by the Kirkwood double-sum formula, and estimated corrections to those results by applying the Zimm rigid-body approximation to a smaller subensemble. They also report that the mobility is linear in X.

Garcia Bernal and co-workers[34] also applied the Zimm rigid-body approximation to ring polymers both in ideal and good solvent conditions,[35] but these were applied to ensembles that were not restricted by knot state. Ensembles of rings that are not restricted by knot state typically contain no knots, especially in good solvents at the chain lengths studied. Therefore, we can safely assume that their good-solvent ensembles contained no knots, although the ideal ensembles probably contained a few.

Gonzalez, Graf, and Maddocks[36] computed the mobility of knots using a rigorous hydrodynamic theory, but these were only for the axial path of maximally inflated knots, rather than for a realistic ensemble of random chains. However, they also report an approximate linearity between mobility and crossing number X.

Brownian dynamics simulation is an additional technique applicable to macromolecules with conformational flexibility, and has been applied by Kanaeda and Deguchi[37] to knotted polymers. With this technique, one simulates the actual configuration-space Brownian motion of a polymer, and therefore obviates the need to apply the Zimm rigid-body approximation. Of necessity, the polymer model is coarse-grained, typically as a beads-and-springs model, and the technique is currently limited to rather short chains. (The Kanaeda–Deguchi study examined chains of 45 segments.) The hydrodynamic interaction is represented at the level of the Oseen or Rotne–Prager tensors. These authors also report linearity between mobility and crossing number X.

More recently, it has been reported that the correlation between electrophoretic mobility and crossing number is reversed at high field strengths, with more complex knots displaying lower mobilities.[11] Weber *et al.*[12,13] performed dynamic Monte Carlo simulations of lattice chains moving past barriers that display a similar effect. At high field strengths, all chains run a higher risk of getting pinned against a barrier, and apparently the more complex knots have a more difficult time climbing over the barrier than do simpler ones. This calculation also serves to display the interesting role of topological entanglements in this problem.

In this paper, we report the application of our own hydrodynamic calculation scheme[22,38–40] to evaluate the transport properties of knotted ring polymers. This technique is equivalent to replacing the Oseen tensor with its scalar average, proportional to $1/r$. Since $1/r$ is the Green's function for the Laplacian, this pre-averaging effectively converts the problem into a boundary-value problem involving Laplace's equation. This latter is solved via path-integration. The apparent error is on the order of 1%–2%. This approach determines the hydrodynamic properties of these rings in solution, and we make no claim that our results are directly applicable to gel transport, although we do find, to within sampling error, linearity between hydrodynamic mobility and X for knotted polymers of fixed length. A major purpose of this paper is to point out interesting properties of both the hydro-

dynamic mobility and of the dilute-solution intrinsic viscosity of random knots, particularly their mass-scaling properties. Our technique also employs the Zimm rigid-body approximation, but its results for each individual rigid-body are expected to be accurate to around 1%.[38] Eleven unique knot states have been investigated. See the companion paper[18] for the full list of knots considered here.

The knot generation technique is described in the companion paper.[18] For the most part, we have concentrated on N_0 values between 100 and 2000. In most cases, ensembles for the calculation of transport properties consisted of 1000 well-annealed specimens.

II. RESULTS FOR THE HYDRODYNAMIC RADIUS AND THE INTRINSIC VISCOSITY

We have calculated the hydrodynamic radius and intrinsic viscosity of eleven different random knots: the unknotted cyclic polymer or "unknot," 3_1 or "trefoil," 4_1, 5_1, 5_2, 6_1, 6_2, 6_3, 9_1, 10_{166} (the last knot to appear in Rolfsen's tabulation[41]), and the (−3,5,7)-pretzel knot (to be referred to hereafter as the "pretzel"). For projections of these knots, see either the companion paper[18] or the tabulations appearing in either Rolfsen's[41] or Adams'[42] books. (The pretzel appears as Fig. 6.25 in Adams.) These knots were modeled both as simple-cubic lattice self-avoiding rings (SARs) to represent good-solvent or swollen conditions, and as SARs with nearest-neighbor contact potential (theta-SARs) to model the theta- or poor-solvent condition.

The hydrodynamic radius is defined either in terms of the hydrodynamic mobility μ,

$$R_h = \frac{1}{6\pi\eta_0\mu}, \tag{1}$$

the diffusion coefficient D,

$$R_h = \frac{kT}{6\pi\eta_0 D}, \tag{2}$$

or the friction coefficient f,

$$R_h = \frac{f}{6\pi\eta_0}, \tag{3}$$

where k is Boltzmann's constant, T is the absolute temperature, and η_0 is the viscosity of the pure solvent. (By the Einstein relationship, all these definitions are equivalent.) The intrinsic viscosity is the leading virial coefficient for the solution viscosity. Two definitions are encountered in the literature, depending on whether one considers a virial expansion in the volume fraction or the mass concentration,

$$\frac{\eta}{\eta_0} = 1 + [\eta]\phi + \cdots, \tag{4a}$$

$$\frac{\eta}{\eta_0} = 1 + [\eta]_P c + \cdots, \tag{4b}$$

where η and η_0 are solution and pure solvent viscosities, respectively, ϕ and c are volume fraction and mass concentration, respectively, and $[\eta]$ and $[\eta]_P$ correspond, respectively, to the two definitions of intrinsic viscosity. ($[\eta]_P$ is the "practical" intrinsic viscosity of experimental polymer science.) Our technique for calculating R_h and $[\eta]_P$, described in detail elsewhere,[22,38–40] is based on the "electrostatic approximation" which is obtained when one replaces the Oseen tensor with its scalar average. At the level of this approximation, R_h and $[\eta]_P$ are directly related to the electrostatic capacity and the electric polarizability tensor, respectively, of a hypothetical perfect conductor having the same size and shape as the macromolecule in question. We have the following relationships:

$$R_h = q_h C, \tag{5}$$

$$m[\eta]_P = V[\eta] = q_\eta \langle\alpha\rangle. \tag{6}$$

Here m and V are, respectively, the mass and volume of the particle, C is the electrostatic capacity, and $\langle\alpha\rangle$ is the mean electric polarizability tensor. The prefactors q_h and q_η are dimensionless shape functionals that depend on the anisotropy of the particle. Accurate determinations of R_h, C, $[\eta]_P$, and $\langle\alpha\rangle$ are the only unequivocal way of determining q_h and q_η in any given case. From such studies,[43–45] we know that

$$q_h = 1.00 \pm 0.01, \tag{7}$$

implying that knowledge of C fixes R_h to within 1%. (We also know that q_h is exactly 1 for arbitrary triaxial ellipsoids.) q_η, on the other hand, is slightly more variable. Nevertheless, exact values are known for arbitrary triaxial ellipsoids, and vary between 0.75 in the disk and elongated ellipsoid limits to $0.833\cdots$ in the sphere limit.[38] It has also been computed for a number of other shapes, and the inequality

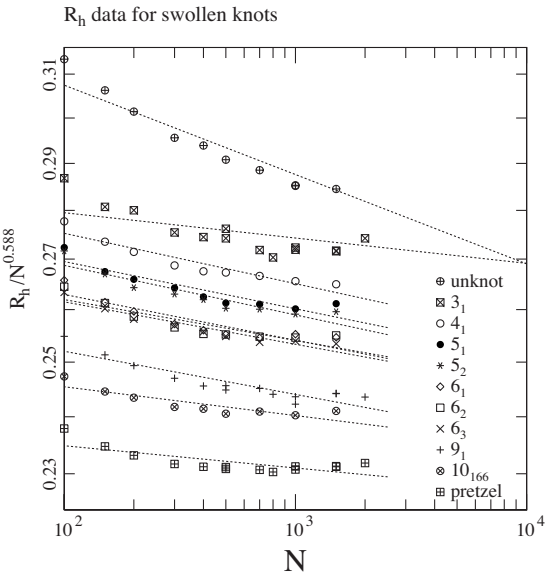

FIG. 1. Mass-scaling of the hydrodynamic radius of swollen knots. Dashed lines are linear least-squares fits.

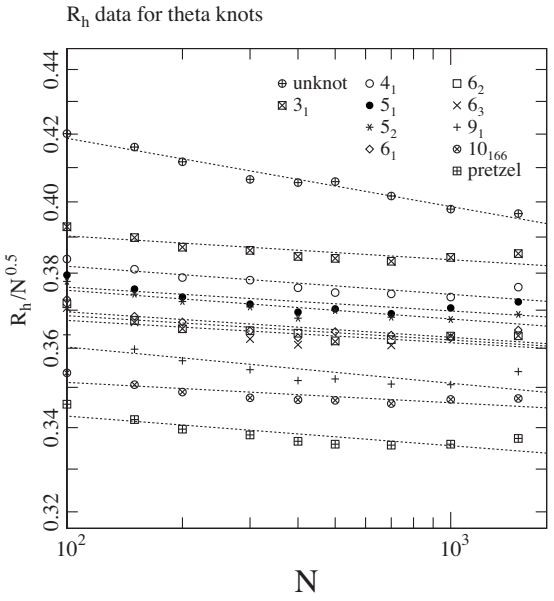

FIG. 2. Mass-scaling of the hydrodynamic radius of theta-state knots. Dashed lines are linear least-squares fits.

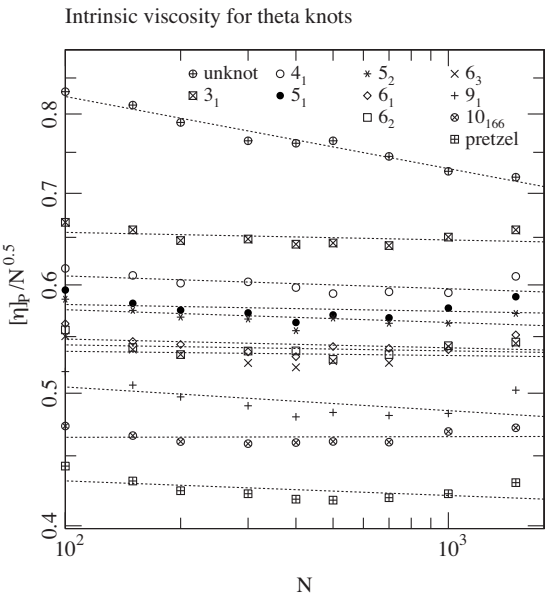

FIG. 4. Mass-scaling of the intrinsic viscosity of theta-state knots. Dashed lines are linear least-squares fits.

$$0.75 \leq q_\eta \leq 0.833\cdots \tag{8a}$$

or

$$q_\eta = 0.79 \times (1.00 \pm 0.05) \tag{8b}$$

appears to hold in general.[43–45] Prior to 2008, our recommended approach for approximating the intrinsic viscosity, at least in the absence of more specific information about q_η, was to employ Eq. (8b), recognizing that the result could be as much as about 5% in error. Since then, we have developed a new approach that determines q_η from anisotropy information available in the complete polarizability tensor.[38] The new approach is numerically exact for all triaxial ellipsoids, and apparently accurate to within about 1% for any object. Unfortunately, much of the data we accumulated on knots were computed prior to this innovation. Nevertheless, applying certain interpolations and extrapolations that are presented in an Appendix, we believe we have a reasonable estimate of the q_η value that would have been obtained had we been able to apply the newer technique in every case.

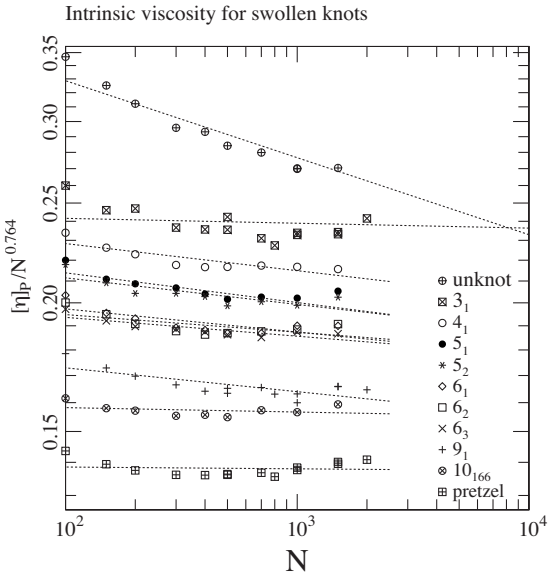

FIG. 3. Mass-scaling of the intrinsic viscosity of swollen knots. Dashed lines are linear least-squares fits.

Log-log plots of the dependence of R_h on N (the ring size) appear in Figs. 1 and 2 for swollen and theta-knots, respectively. Figures 3 and 4 display our results for $[\eta]_P$, again for swollen-state and for theta-state knots, respectively. $[\eta]_P$ is determined from Eq. (6) by assuming that each segment has unit mass: $m=N$.

Under conditions for which the radius of gyration obeys the scaling law,

$$R_g \sim N^\nu, \tag{9}$$

where ν is the "metric" exponent, then naive scaling arguments predict

$$R_h \sim N^\alpha, \quad \alpha = \nu \tag{10}$$

and

TABLE I. Effective mass-scaling exponents for the hydrodynamic radius.

	α swollen	Δ_α swollen	α theta	Δ_α theta
Unknot	0.559	−0.03	0.479	−0.03
3_1	0.580	−0.05	0.493	−0.05
4_1	0.572	−0.07	0.491	−0.05
5_1	0.573	−0.07	0.493	−0.05
5_2	0.572	−0.07	0.491	−0.06
6_1	0.573	−0.07	0.492	−0.05
6_2	0.575	−0.07	0.492	−0.06
6_3	0.574	−0.07	0.493	−0.06
9_1	0.574	−0.06	0.489	−0.05
10_{166}	0.579	−0.08	0.494	−0.06
"Pretzel"	0.581	−0.07	0.491	−0.04

TABLE II. Effective mass-scaling exponents for the intrinsic viscosity.

	β swollen	Δ_β swollen	β theta	Δ_β theta
Unknot	0.689	−0.08	0.447	−0.08
3_1	0.759	−0.14	0.494	−0.13
4_1	0.738	−0.19	0.491	−0.14
5_1	0.739	−0.20	0.495	−0.14
5_2	0.738	−0.20	0.491	−0.15
6_1	0.742	−0.19	0.494	−0.14
6_2	0.747	−0.20	0.496	−0.14
6_3	0.746	−0.20	0.497	−0.15
9_1	0.741	−0.17	0.483	−0.13
10_{166}	0.760	−0.21	0.500	−0.15
"Pretzel"	0.762	−0.18	0.489	−0.13

$$[\eta] \sim [\eta]_P \sim N^\beta, \quad \beta = 3\nu - 1. \tag{11}$$

However, the most notable aspect of the data in Figs. 1–4 is the systematic deviation away from linearity, which obviously indicates that Eqs. (10) and (11) are not satisfied by these knots. Figures 1–4 actually display $R_h/N^{0.588}$, $R_h/N^{0.5}$, $[\eta]_P/N^{0.764}$, or $[\eta]_P/N^{0.5}$, which accentuates departures from the naive power-law scaling. In spite of these obvious departures from the "universal" mass-scaling laws, we tabulate effective α and β exponents, determined by least-squares fits, in order to characterize general trends in the data. These appear in Tables I and II. We also define the following two indices, which quantify departures from naive scaling:

$$\Delta_\alpha = \alpha - \nu, \tag{12}$$

$$\Delta_\beta = \beta - (3\nu - 1). \tag{13}$$

As can be seen in the figures and tables, the N-dependence of unknots differs from that of true knots, at least in the range of N studied, and we summarize these trends in Table III.

Can we explain the discrepancy between our results and the anticipated scaling laws? Our experience concerning both the R_g behavior of random knots[18] and the transport properties of linear polymers[46,47] indicates that the transport properties of random knots exhibit a "double" cross-over, i.e., we are seeing the result of more than one cross-over effect. Indeed, the evidence is strong that the scaling laws of Eqs. (9)–(11) will only be observed at extremely large N, so large, in fact, that it probably exceeds both the chain lengths of typical synthetic polymers and the chain lengths of simulated polymers that are currently accessible. (Whether or not extremely large DNAs are in the asymptotic domain is an open question. A study of the transport properties of stiff chains such as DNA will be published shortly.[55(a)]) One of these cross-overs is the transition from delocalized to localized knotting,[15,18,25–30] which implies that Eq. (9) is not followed exactly at typical chain lengths. The second cross-over results from the so-called "draining" phenomenon, observed in linear polymers,[46,47] in which transport properties continue to exhibit dependence on local properties even at very large N. Draining is a consequence of the ability for solvent flow to penetrate significantly into the region of space occupied by the object, and the cross-over effect originates because this penetration achieves its large-N limit only very slowly.

We are able to rationalize all the trends seen in Table III. The values of the effective ν exponents for unknots, 0.59 and 0.51 for swollen and theta unknots, respectively, are a consequence, as explained in the companion paper, of the fact that at these values of N, the ensemble that contains rings of all possible knot states is dominated by unknots. Therefore, until N becomes very large, we expect ensembles of unknots to display the same exponents as unrestricted ensembles, namely, $\cong$0.59 and 0.5, respectively; the two ensembles are practically identical. The fact that effective ν exponents for knots, $\approx$0.64 and $\approx$0.54 for swollen and theta-knots, respectively, are greater than the exponents for unknots is consistent with an inequality discussed in the companion paper, which states that R_g is a stronger function of N for any one particular knot state than it is for ensembles containing all knot states. Finally, the trends in α and β, as quantified in Δ_α and Δ_β, are consistent with what we now know about the draining phenomenon. $\Delta_\alpha \approx -0.03$ to -0.05 and $\Delta_\beta \approx 3\Delta_\alpha$ are typical for flexible linear polymer models in this range of lengths, and indicate that the polymers are becoming more draining, i.e., as $N \to \infty$ they are more and more effectively penetrated by solvent during transport.[47]

The last line in Table III displays what we believe are the correct asymptotic values for the exponents of both swollen and theta-knots. The lack of direct empirical evidence means that these values are conjectural. However, there are two good reasons for believing them. First, the most common expectation in the literature, borne out by extrapolations of existing Monte Carlo data,[18,30,48–53] is that rings confined to a given knot state will eventually conform to Eq. (9) at sufficiently large N, and that they will do so with $\nu = \nu_{\mathrm{SAW}}$, where $\nu_{\mathrm{SAW}} \cong 0.588$ is the exponent expected of linear self-avoiding walks. (Interestingly, this same exponent is expected both for sufficiently long knotted SARs and theta-SARs.) Second, if Eq. (9) does hold asymptotically, then Eqs. (10) and (11) must also be asymptotically true with $\alpha = \nu_{\mathrm{SAW}}$, and $\beta = 3\nu_{\mathrm{SAW}} - 1$, since there is no other relevant length scale.

TABLE III. Overall trends in effective exponents.

	ν	α	β	Δ_α	Δ_β
Swollen unknots	0.59	0.56	0.69	−0.03	−0.08
Swollen knots	≈0.64	≈0.58	≈0.75	≈−0.06	≈−0.17
Theta unknots	0.51	0.48	0.45	−0.03	−0.08
Theta-knots	≈0.54	≈0.49	≈0.49	≈−0.05	≈−0.13
Asymptotes	0.59	0.59	0.76	0	0

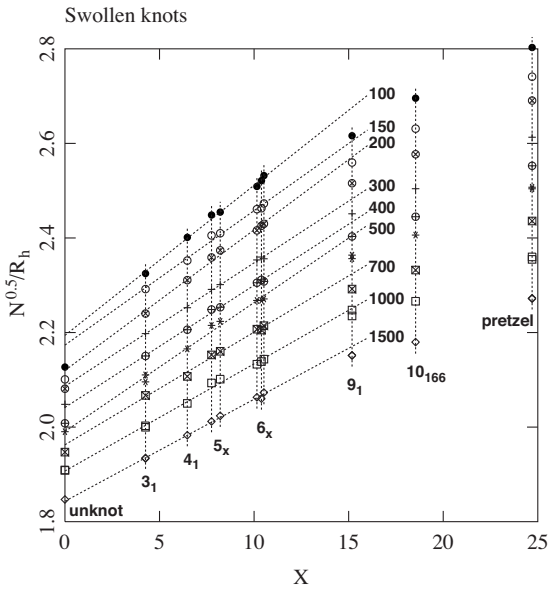

FIG. 5. Correlations between hydrodynamic mobility (proportional to $1/R_h$) and average crossing number X for swollen knots. The seven knots between 3_1 and 6_x are linearly correlated (dashed lines) at all N values examined.

III. MOBILITY-CROSSING NUMBER CORRELATIONS

We now investigate correlations between mobility and average crossing number X. As shown in Eq. (1), the hydrodynamic mobility is inversely proportional to the hydrodynamic radius. Figures 5 and 6 display $N^{0.5}/R_h$ versus X and $N^{0.4}/R_h$ versus X for swollen and for theta-state knots, respectively. (Normalization by $N^{0.5}$ or $N^{0.4}$ has been done for readability.) The dashed lines are linear least-squares fits for the seven knots 3_1, 4_1, 5_1, 5_2, 6_1, 6_2, and 6_3, and as can be seen, these seven knots display linear correlations to within sampling error at any value of N. However, at the lower N values, these lines do not predict the hydrodynamic mobilities of any of the other knots: the unknot, 9_1, 10_{166} or the pretzel, although at the largest N values studied, 1000 and 1500, these lines do become accurate predictors of the behavior of at least unknots and of 9_1.

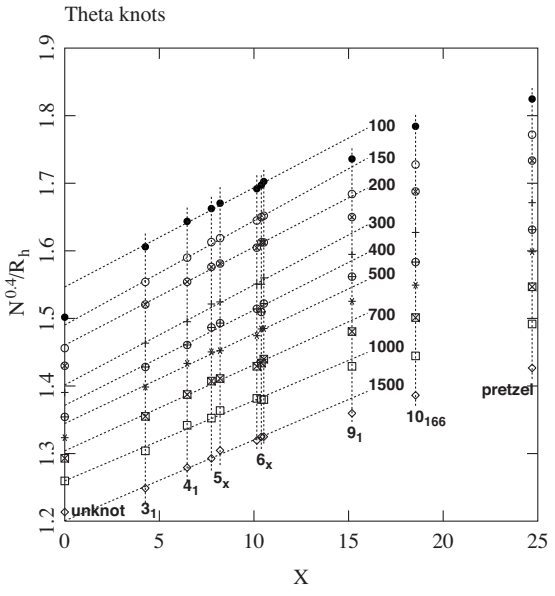

FIG. 6. Same as Fig. 5 for theta-state knots.

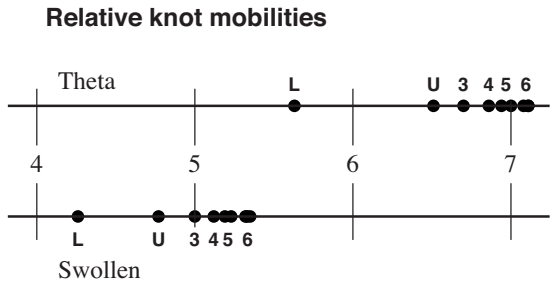

FIG. 7. Relative hydrodynamic mobilities of linear chains L, unknotted ring chains U, and of the knots of the indicated numbers of crossings, on an arbitrary scale, as predicted by our calculations. In contrast, empirical electrophoretic mobilities of linear chains are often larger than those of unknots and of at least some of the knots.

The empirical correlations for DNA knots are reported to involve this list of 13 knots: the unknot, 3_1, 4_1, 5_1, 5_2, 6_1, "granny" (a pairwise composite of 3_1 knots), 7_1, 7_2, 8_1, 9_1, 9_2, and 10_1, and seven of those are included in this study. They are also reported to involve cyclic DNAs of 7000 basepairs.[7,8,10] The size of the cyclic DNAs in these electrophoresis experiments is relevant because our results, as displayed in Figs. 5 and 6, indicate that the quality of the linear relationship depends on chain length.

A further complication is that hydrodynamic models of chain transport are unable to predict the mobilities of linear DNAs relative to those of knotted DNA. Crisona *et al.*[7] examined plasmids of length about 5 kb, and reported that the electrophoretic mobility of linear chains is intermediate between that of cyclic unknots and cyclic trefoils, i.e., 3_1 knots. Arsuaga *et al.*,[54] in a study of P4-phage DNA, report that the linear chains drift with mobilities intermediate between the five- and six-crossing knots. This is *not* the behavior expected of the hydrodynamic mobility: the less compact linear chains are expected to have lower mobilities than either the unknot or any of the knots. Figure 7 displays our predictions for the hydrodynamic mobilities of linear chains relative to knotted chains, and should be compared with Fig. 7 of Ref. 7, Fig. 1 of Ref. 10, or Fig. 2 of Ref. 54. (Our computations for equivalent linear chains are reported in Ref. 47.) Obviously, the relative electrophoretic mobilities of linear, unknotted cyclic, and knotted cyclic DNAs indicate that the gel does not act as an effective hydrodynamic medium in these measurements. Undoubtedly, there is a complex interplay between chain length, pore size, chain topology, and other aspects of the gel structure. There is a clear need for an improved theory of polymer separation by gels.

IV. DIMENSIONLESS RATIOS

Additional evidence for the draining cross-over is seen in the chain-length dependence of certain dimensionless ratios. These ratios are also of interest, because they combine the results of several experiments to extract shape-dependent information. The ratio R_h/R_g is shown in Figs. 8 and 9 for swollen and theta-knots, respectively. Asymptotically, we do expect R_h to scale as R_g, but as long as R_h/R_g displays an explicit chain-length dependence, we are not in the asymptotic domain. The value of this ratio for 10_{166} and the pretzel knot at $N=100$ approaches the value for hard spheres,

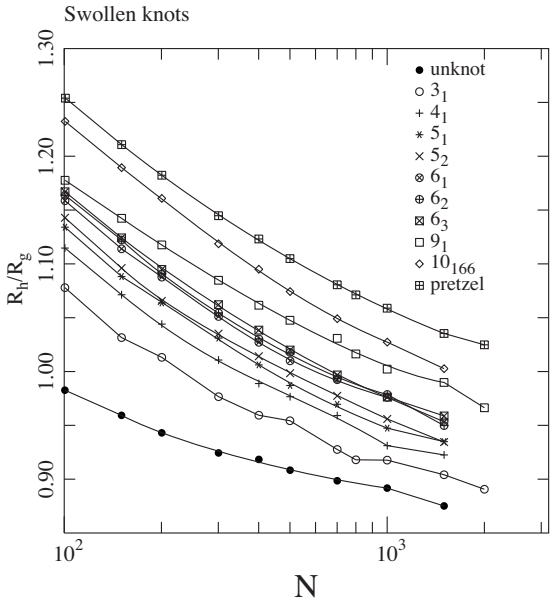

FIG. 8. N-dependence of the ratio R_h/R_g for swollen knots.

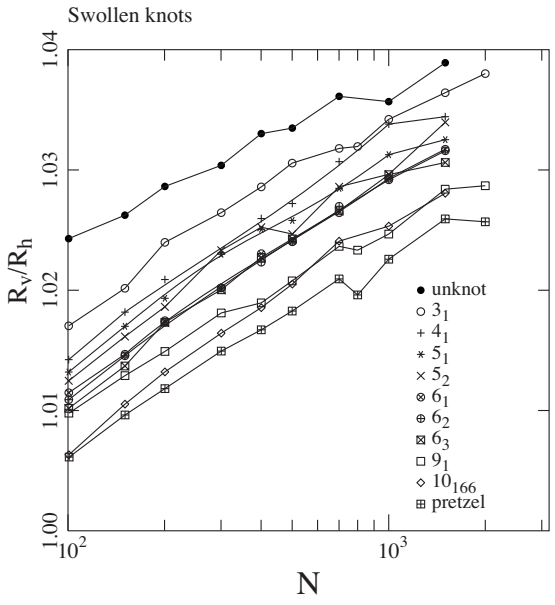

FIG. 10. N-dependence of the ratio R_v/R_g for swollen knots.

$(5/3)^{1/2} \cong 1.29$. $N=100$ is only 35% larger than $n_{\min}=74$, the smallest possible N for the pretzel knot on this lattice,[18] which indicates that the structure is closer to a globule than a random coil, which in turn explains why R_h/R_g approaches a value comparable to a sphere. Apparently, R_h/R_g is monotone-decreasing for all knots, but decreases more strongly for swollen than for theta-knots. We know that for the equivalent linear chains, $R_h/R_g \to 0.70$ and 0.79, respectively, for long swollen and theta-state polymers, as $N \to \infty$.[47] It is unlikely that ring polymers will exhibit those same asymptotes because knots should become localized as $N \to \infty$. We therefore expect all knot states to eventually reach the same asymptotic ratio, independent of knot state.

It is also possible to form a dimensionless ratio combining the intrinsic viscosity and the hydrodynamic radius. In order to do this, we first define the viscosity radius, which is taken to be the radius of the effective sphere having the same product of $[\eta]_P$ and mass m as the polymer. Therefore, it obeys

$$R_v = \left(\frac{3m[\eta]_P}{10\pi} \right)^{1/3}. \tag{14}$$

Figures 10 and 11 show R_v/R_h for swollen and theta-knots, respectively. This ratio also proves to be an indicator of the anisotropy of the particle. R_v/R_h is exactly 1 for spheres, and we note that this value is approached by the complex knots (10_{166} and the pretzel, especially) at low N. R_v/R_h is known to be within about 10% of 1 for all but highly elongated objects[55(b)] and even these weak trends in the vicinity of 1 are indicators of anisotropy. R_v/R_h indicates, therefore, that all knots are more anisotropic at either larger N or for the simpler topologies. This is consistent with expectations,

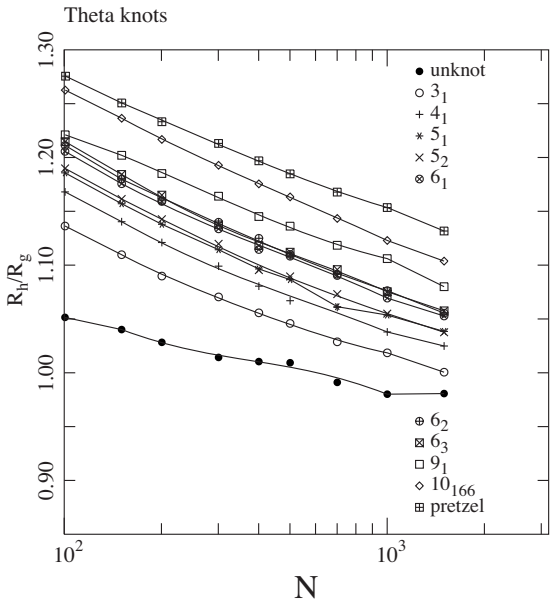

FIG. 9. N-dependence of the ratio R_h/R_g for theta-state knots.

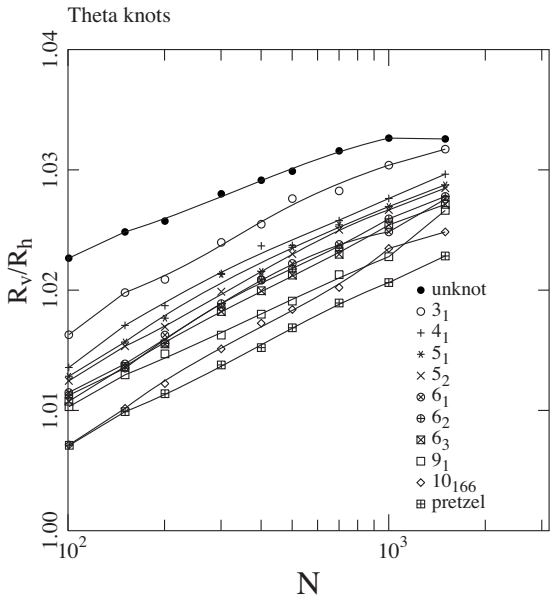

FIG. 11. N-dependence of the ratio R_v/R_g for theta-state knots.

since as already noted, the more complex knots are expected to be practically globular when $N \approx 100$. It is also consistent with findings by Rawdon *et al.*[56] and by Millett *et al.*[57] who examined other anisotropy measures of knotted polymers. The N-dependence of this ratio is another indication of the draining cross-over, since we expect $R_v/R_h \sim N^0$ in the asymptotic domain.

V. CONCLUSIONS

Much effort has gone into explaining the relative electrophoretic mobilities of DNA knots through purely hydrodynamic theories, or other approaches which do not explicitly include the gel.[8,10,21,23,24,36] However, because the hydrodynamic theories are unable to explain the relative electrophoretic mobilities of linear and knotted polymers in some measurements, we do not believe that hydrodynamic theory provides a reliable description of gel-electrophoretic transport of these DNA molecules. The dynamic Monte Carlo simulation studies of Weber *et al.*,[12,13] that model knotted chain transport past grids, are probably more realistic at capturing the effect of the gel.

The hydrodynamic mobility and the intrinsic viscosity of knotted ring polymers are nevertheless interesting and notable. They provide an interesting example of the failure of mass-scaling laws, at least at typical molecular masses. The transport properties of ring polymers restricted to a single knot state appear to be in a double cross-over, although the lack of empirical evidence means that this is at least somewhat conjectural. The metric properties, e.g., radius of gyration, do not become universal until the chain length is large enough for the knot to become well-localized.[15,18,25–30] But because of the draining phenomenon,[46,47] the transport properties also do not become universal until chains are extremely long. Every indication is that when sufficiently long, knotted ring polymers confined to a specific knot state will exhibit universal mass-scaling, and as summarized in this and the companion paper[18] there are good reasons to expect the exponents that are given in the last row of Table III. However, adequate experimental or simulation evidence is still lacking.

APPENDIX: REFINED ESTIMATES OF q_η

The greater portion of the intrinsic viscosity results was obtained before the innovation described in Ref. 38, at which time Eq. (8a) was our best estimate for the parameter q_η. Here we describe the approach we employed to estimate improved values of q_η for all of these earlier results. Because a few ensembles of swollen knots were evaluated at a later date using the improved approach, the q_η values labeled "swollen knots" in Fig. 12 are available. (These ensembles include unknots, the knots 3_1, 9_1, and pretzel knots, for which $C=0,3,9$, and 15, respectively, at the indicated N values.) The q_η values for these knots are obviously correlated with both N and C. The following expression is the linear least-squares fit to these data points, taking $\log_{10} N$ and C as the independent variables,

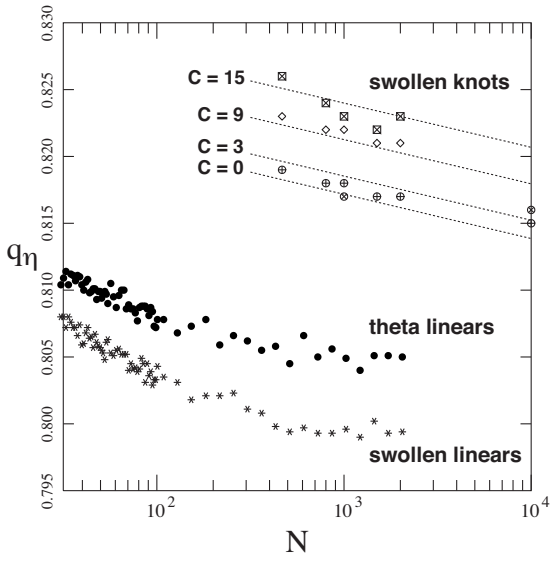

FIG. 12. Dependence of the intrinsic viscosity prefactor q_η on N for the indicated models. These data are used to determine the approximations of Eqs. (A1) and (A2).

$$q_\eta = 0.8271 - (3.31 \times 10^{-3}) \log_{10} N + (4.55 \times 10^{-4}) \quad C(\text{swollen knots}). \tag{A1}$$

No theta-knots were evaluated by the newer q_η technique, but as reported in Ref. 47, we do have data on the equivalent linear chains, which also appear in Fig. 12. q_η values for linear theta chains are displaced upward by about 0.005 relative to the swollen linears. Assuming the same displacement can be applied for theta-knots, we obtain

$$q_\eta = 0.8321 - (3.31 \times 10^{-3}) \log_{10} N + (4.55 \times 10^{-4}) C(\text{theta knots}). \tag{A2}$$

Equations (A1) and (A2) were employed to correct all of the earlier intrinsic viscosity data. Note that all the relevant q_η values for both swollen and theta-knots are in the vicinity of 0.82 ± 0.01, so that merely by using 0.82 in place of 0.79 would have constituted a significant improvement. The additional correction provided by Eq. (A1) or Eq. (A2) really only applies to the third decimal digit. We emphasize that Eqs. (A1) and (A2) are intended to approximate the q_η values that would have been determined for these calculations had the later approach been available.

[1] F. B. Dean, A. Stasiak, T. Koller, and N. R. Cozzarelli, J. Biol. Chem. **260**, 4975 (1985).
[2] S. A. Wasserman, J. M. Dungan, and N. R. Cozzarelli, Science **229**, 171 (1985).
[3] S. A. Wasserman and N. R. Cozzarelli, Science **232**, 951 (1986).
[4] D. W. L. Sumners, Proc. Symp. Appl. Math. **45**, 39 (1992).
[5] S. Y. Shaw and J. C. Wang, Science **260**, 533 (1993).
[6] J. M. Sogo, A. Stasiak, M. L. Martinez-Robles, D. B. Krimer, P. Hernandez, and J. B. Schvartzman, J. Mol. Biol. **286**, 637 (1999).
[7] N. J. Crisona, R. Kanaar, T. N. Gonzalez, E. L. Zechiedrich, A. Klippel, and N. R. Cozzarelli, J. Mol. Biol. **243**, 437 (1994).
[8] A. Stasiak, V. Katritch, J. Bednar, D. Michoud, and J. Dubochet, Nature (London) **384**, 122 (1996).
[9] L. Martin-Parras, I. Lucas, M. L. Martinez-Robles, P. Hernandez, D. B. Krimer, O. Hyrien, and J. B. Schvartzman, Nucleic Acids Res. **26**, 3424 (1998).
[10] A. V. Vologodskii, N. J. Crisona, B. Laurie, P. Pieranski, V. Katritch, J.

Dubochet, and A. Stasiak, J. Mol. Biol. **278**, 1 (1998).
[11] S. Trigueros, J. Arsuaga, M. E. Vazquez, D. W. Sumners, and J. Roca, Nucleic Acids Res. **29**, e67 (2001).
[12] C. Weber, A. Stasiak, P. De los Rios, and G. Dietler, J. Phys.: Condens. Matter **18**, S161 (2006).
[13] C. Weber, A. Stasiak, P. De los Rios, and G. Dietler, Biophys. J. **90**, 3100 (2006).
[14] A. Stasiak, J. Dubochet, V. Katritch, and P. Pieranski, in *Ideal Knots*, edited by A. Stasiak, V. Katritch, and L. H. Kauffman (World Scientific, New York, 1999), pp. 1–19.
[15] A. Yu. Grosberg, A. Feigel, and Y. Rabin, Phys. Rev. E **54**, 6618 (1996).
[16] V. Katritch, J. Bednar, D. Michoud, R. G. Scharein, J. Dubochet, and A. Stasiak, Nature (London) **384**, 142 (1996).
[17] Homepage of Professor P. Pieranski, Poznan University of Technology, Poznan, Poland, fizyka.phys.put.poznan.pl/~pieransk/.
[18] M. L. Mansfield and J. F. Douglas, J. Chem. Phys. **133**, 044903 (2010).
[19] H. Yamakawa, *Modern Theory of Polymer Solutions* (Harper & Row, New York, 1971).
[20] M. Doi and S. F. Edwards, *The Theory of Polymer Dynamics* (Oxford University Press, Oxford, 1986).
[21] Y.-J. Sheng and H.-K. Tsao, J. Chem. Phys. **116**, 10523 (2002).
[22] M. L. Mansfield, J. F. Douglas, S. Irfan, and E.-H. Kang, Macromolecules **40**, 2575 (2007).
[23] D. W. Matuschek and A. Blumen, Macromolecules **22**, 1490 (1989).
[24] C. A. Croxton and R. M. Turner, Macromolecules **24**, 177 (1991).
[25] E. Guitter and E. Orlandini, J. Phys. A **32**, 1359 (1999).
[26] V. Katritch, W. K. Olson, A. Vologodskii, J. Dubochet, and A. Stasiak, Phys. Rev. E **61**, 5545 (2000).
[27] B. Marcone, E. Orlandini, A. L. Stella, and F. Zonta, J. Phys. A **38**, L15 (2005).
[28] Y. Kantor, Pramana, J. Phys. **64**, 1011 (2005).
[29] E. Ercolini, F. Valle, J. Adamcik, G. Witz, R. Metzler, P. De Los Rios, J. Roca, and G. Dietler, Phys. Rev. Lett. **98**, 058102 (2007).
[30] E. Orlandini and S. G. Whittington, Rev. Mod. Phys. **79**, 611 (2007).
[31] C. A. Croxton, J. Phys. A **17**, 2129 (1984).
[32] B. H. Zimm, Macromolecules **13**, 592 (1980).
[33] V. V. Rybenkov, A. V. Vologodskii, and N. R. Cozzarelli, J. Mol. Biol. **267**, 299 (1997).
[34] J. M. Garcia Bernal, M. M. Tirado, J. J. Freire, and J. Garcia de la Torre, Macromolecules **23**, 3357 (1990).
[35] J. M. Garcia Bernal, M. M. Tirado, J. J. Freire, and J. Garcia de la Torre, Macromolecules **24**, 593 (1991).
[36] O. Gonzalez, A. B. A. Graf, and J. H. Maddocks, J. Fluid Mech. **519**, 133 (2004).
[37] N. Kanaeda and T. Deguchi, Phys. Rev. E **79**, 021806 (2009).
[38] M. L. Mansfield and J. F. Douglas, Phys. Rev. E **78**, 046712 (2008).
[39] M. L. Mansfield, J. F. Douglas, and E. J. Garboczi, Phys. Rev. E **64**, 061401 (2001).
[40] E.-H. Kang, M. L. Mansfield, and J. F. Douglas, Phys. Rev. E **69**, 031918 (2004).
[41] D. Rolfsen, *Knots and Links* (Publish or Perish, Berkeley, CA, 1976).
[42] C. C. Adams, *The Knot Book: An Elementary Introduction to the Mathematical Theory of Knots* (Freeman, New York, 1994).
[43] J. B. Hubbard and J. F. Douglas, Phys. Rev. E **47**, R2983 (1993).
[44] J. F. Douglas and E. J. Garboczi, Adv. Chem. Phys. **91**, 85 (1995).
[45] J. F. Douglas, Adv. Chem. Phys. **102**, 121 (1997).
[46] B. Dünweg, D. Reith, M. Steinhauser, and K. Kremer, J. Chem. Phys. **117**, 914 (2002).
[47] M. L. Mansfield and J. F. Douglas, Phys. Rev. E **81**, 021803 (2010).
[48] E. J. Janse van Rensburg and S. G. Whittington, J. Phys. A **24**, 3935 (1991).
[49] E. Orlandini, M. C. Tesi, E. J. Janse van Rensburg, and S. G. Whittington, J. Phys. A **31**, 5953 (1998).
[50] M. K. Shimamura and T. Deguchi, Phys. Rev. E **64**, 020801(R) (2001).
[51] M. K. Shimamura and T. Deguchi, Phys. Rev. E **65**, 051802 (2002).
[52] M. K. Shimamura and T. Deguchi, J. Phys. A **35**, L241 (2002).
[53] A. Dobay, J. Dubochet, K. Millett, P.-E. Sottas, and A. Stasiak, Proc. Natl. Acad. Sci. U.S.A. **100**, 5611 (2003).
[54] J. Arsuaga, M. Vazquez, P. McGuirk, S. Trigueros, D. W. Sumners, and J. Roca, Proc. Natl. Acad. Sci. U.S.A. **102**, 9165 (2005).
[55] (a) M. L. Mansfield and J. F. Douglas, "Is duplex DNA a swollen random coil?"(in preparation); (b) M. L. Mansfield and J. F. Douglas, "Scale variant indicators of particle shape (in preparation).
[56] E. Rawdon, J. C. Kern, M. Piatek, P. Plunkett, A. Stasiak, and K. C. Millett, Macromolecules **41**, 8281 (2008).
[57] K. C. Millett, P. Plunkett, M. Piatek, E. J. Rawdon, and A. Stasiak, J. Chem. Phys. **130**, 165104 (2009).